Noname manuscript No.
(will be inserted by the editor)

Onset of Convection in a Triangular Porous Prism with Robin-Type Thermal Wall Condition

Peder A. Tyvand · Jonas Kristiansen Nøland

Received: date / Accepted: date

Abstract This paper investigates a peculiar case of thermal convection in a vertical porous prism with impermeable and partially conducting walls. We facilitate the analysis in the numerical finite element environment alongside with analytical considerations, in special cases where direct solutions are feasible. The present eigenvalue problem results in a non-normal mode behaviour in the horizontal cross-sectional plane. Further, it is identified that the stagnation points for the horizontal flow are displaced from the extremal points of the temperature perturbation, for both symmetric and antisymmetric eigenfunctions. In addition, the corresponding normal-mode counterparts are provided from an analogy solution. We show that the critical Rayleigh number decreases with increasing Robin parameter values for all of the investigated aspect ratios. Finally, the influence of the aspect ratio on the critical Rayleigh number for the fully conducting wall case is identified. An asymptotic benchmark case of the Robin condition is validated from well known analytical solutions which confirms the effectiveness of the predictions made in this paper. In fact, this is the first contribution that reports a three-dimensional geometry with a two-dimensional non-normal mode.

Keywords Convection · Cylinder · Porous medium · Vertical cylinder

P.A. Tyvand
Faculty of Mathematical Sciences and Technology
Norwegian University of Life Sciences
1432 Ås, Norway
Tel: +47-67231564 E-mail: Peder.Tyvand@nmbu.no

J.K. Nøland (Corresponding Author)
Faculty of Information Technology and Electrical Engineering
Norwegian University of Science and Technology
E-mail: Jonas.k.Noland@ntnu.no

1 Introduction

The Horton-Rogers-Lapwood (HRL) problem for the onset of convection in a horizontal porous layer has a two-dimensional (2D) structure for the mathematical solution, even though the physical problem is 3D. The general solution is a superposition of individual 2D Fourier modes (Horton and Rogers [1], Lapwood [2]). Any Fourier mode of convection onset is 2D in a vertical (x, z) plane aligned with its wave number vector. This is a trivial degeneracy in dimension due to the lack of boundaries in the horizontal plane.

The HRL problem has two types of degeneracy. (i) The solution in the vertical direction is a normal mode. (ii) A Fourier element of the solution in the horizontal direction is by definition a normal mode. Since normal modes are governed by a second-order equation, these degeneracies are essentially reductions from 4th order to 2nd order for the full eigenvalue problem.

The challenges of bringing more generality and physical realism into the HRL solution are two-fold: (1) To provide the need for a 3D solution, by considering a finite 3D porous medium. A vertical cylinder is a natural case to consider (Wooding [3]). (2) To provide mathematical solutions that are not of the normal-mode type. Any solution that is not of normal-mode type confirms that the eigenvalue problem is a genuine fourth-order problem. As soon as a normal-mode type of solution applies, the problem reduces to an essentially second-order problem. A number of papers have been written on porous cylinders, with normal modes as the natural starting point. Beck [4] and Zebib [5] carried out the details of the theory by Wooding [3], for a rectangular box and a circular cylinder, respectively. Wooding [3] had pointed out the necessity of degeneration in the boundary condition, where thermal and mechanical conditions coincide mathematically.

Tyvand and Storesletten [6] developed from first principles the restrictions for the normal-mode class of solutions for vertical cylinders. They solved the problem of a vertical cylinder with a triangular cross-section. Only the simple case of a right-angle isosceles cylinder was considered. The equilateral triangle is another cross-section for which exact analytical eigenfunctions can be found of the Helmholtz equation. This more complicated solution is known from the theory of vibrating membranes in elasticity. Barletta and Storesletten [7] have written the only paper where a cylinder with an elliptical cross-section has been studied. For mathematical convenience, they chose the Dirichlet conditions of open/conducting cylinder walls instead of the classical case of impermeable/insulating cylinder walls.

There exists only a handful of papers that treat the onset problem in a 3D porous medium where the normal-mode type of spatial dependence is challenged. Haugen and Tyvand [8] wrote the first paper on a vertical porous cylinder full-normal dependency in the radial direction of the circular cross-section. This model was generalized by Nygård and Tyvand [9] to account for partial conduction and partial penetration at the cylinder walls. In the present paper, we study the same type of model for a triangular cylinder, with the Robin-type condition of partially conducting cylinder walls.

Our problem contrasts the circular cross-sections, where the azimuthal separability of the eigenfunctions restricts the non-normal mode dependency to the 1D radial direction only. Non-normal modes in 1D can be studied analytically. Our triangular cross-section results in 2D non-normal modes that cannot be separated in space, where no analytical methods are known.

The study of 1D non-normal modes for the HRL problem started with Nield [10] who solved the onset problem with all possible Dirichlet and/or Neumann conditions for the temperature perturbation and the vertical velocity at the lower and upper boundaries. Barletta *et al.* [11] extended Nield's analysis for the HRL problem by allowing general Robin conditions at the lower and upper boundaries. 2D non-normal modes for the HRL problem is a new challenging topic. Tyvand *et al.* [12] has solved a 2D problem of non-normal modes in a vertical rectangle. In the present paper, we carry this type of analysis further by considering a fully 3D problem of a vertical cylinder, with normal-mode dependency in the vertical direction. By spatial separation, we will have a non-normal modes dependency the horizontal cross-section plane.

The significance of the present paper is that it is the first theoretical study of a three-dimensional Darcy-Bénard eigenvalue problem with full non-normal dependency over the horizontal cross-section of a cylinder. The present type of modeling has the disadvantage that no analytical solution methods are known. The advantage is that more physical realism can be included in the boundary conditions, compared with the implicit degeneracy of the existing models based on normal modes.

2 Mathematical formulation

A three-dimensional porous medium is bounded by horizontal planes $z = -h/2$ and $z = h/2$. The porous medium is homogeneous and isotropic. Cartesian coordinates (x, y, z) are introduced. The z axis is directed vertically upwards. We will consider a vertical cylinder, noting that the linear theory has been established both for impermeable insulating walls (Wooding [3]), and for open conducting walls (Barletta and Storesletten [7]). We will here develop the general linear theory for vertical cylinders with impermeable and thermally conducting walls, and we will perform calculations for the case of an isosceles triangular cylinder. We will allow a thermal Robin condition for the cylinder wall, whereby the standard case of impermeable adiabatic walls (Wooding [3]) arises as a limit case.

The velocity vector $\mathbf{v}$ has Cartesian components (u, v, w). The temperature field is represented as $T(x, y, z, t)$ with t denoting time. In the undisturbed state, the lower plane $z = -h/2$ is kept at a constant temperature $T = T_0$, and the upper plane $z = h/2$ is kept at a constant temperature $T = T_0 - \Delta T$. Here ΔT is a positive temperature difference. The gravitational acceleration g is written in vector form as $\mathbf{g}$.

The standard Darcy-Boussinesq equations for free thermal convection in a porous medium can be written

$$\nabla P + \frac{\mu}{K}\mathbf{v} + \rho_0 \beta\ (T - T_0)\mathbf{g} = 0, \tag{1}$$

$$\nabla \cdot \mathbf{v} = 0, \tag{2}$$

$$(\rho c_p)_m \frac{\partial T}{\partial t} + (\rho c_p)_f\ \mathbf{v} \cdot \nabla T = \lambda_m \nabla^2 T. \tag{3}$$

In these equations, P is the dynamic pressure, β is the coefficient of thermal expansion, $\rho = \rho_0$ is the fluid density at the reference temperature T_0, μ is the dynamic viscosity of the saturating fluid, K is the permeability, c_p is the specific heat at constant pressure, and λ_m is the thermal conductivity of the saturated porous medium. The subscript m refers to an average over the solid/fluid mixture, while the subscript f refers to the saturating fluid alone.

The lower and upper boundaries support a given temperature difference ΔT across the porous layer. The undisturbed basic state of pure conduction has the boundary temperatures

$$T = T_0 + \Delta T, \quad \text{at} \quad z = 0 - h/2, \tag{4}$$

$$T = T_0, \quad \text{at} \quad z = h/2. \tag{5}$$

T_0 is a reference temperature. These boundary temperatures will be maintained also when the basic state is disturbed with infinitesimal perturbations.

The kinematic conditions for the impermeable lower and upper boundaries are

$$w = 0, \quad \text{at} \quad z = -h/2, \tag{6}$$

$$w = 0, \quad \text{at} \quad z = h/2. \tag{7}$$

Figure 1 shows definition sketches for a vertical enclosure with the triangular cross-section which will be our calculated example.

2.1 Dimensionless equations

From now on we work with dimensionless variables. We reformulate the mathematical problem in dimensionless form by means of the transformations

$$\begin{gathered} \frac{1}{h}(x,z) \to (x,z), \qquad \frac{h}{\kappa_m}(u,v,w) \to (u,v,w), \qquad h\nabla \to \nabla, \\ \frac{1}{\Delta T}(T - T_0) \to T, \qquad \frac{K}{\mu \kappa_m}(P - P_0) \to P, \qquad \frac{(\rho c_p)_f \kappa_m}{(\rho c_p)_m h^2} t \to t, \end{gathered} \tag{8}$$

where $\kappa_m = \lambda_m/(\rho_0 c_p)_f$ is the thermal diffusivity of the saturated porous medium. We denote the vertical unit vector by $\mathbf{k}$, directed upwards.

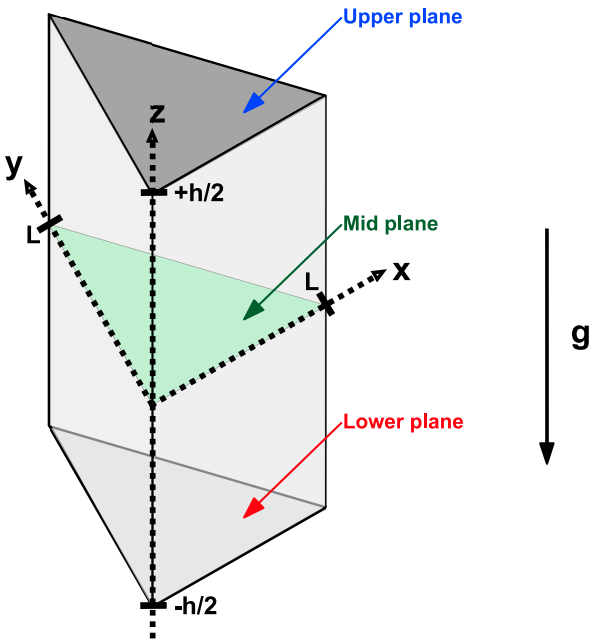

Fig. 1 Definition sketch of a vertical porous enclosure with triangular cross-section. The investigated mid plane is indicated.

The dimensionless governing equations can then be written

$$\mathbf{v} + \nabla P - RT\mathbf{k} = 0. \tag{9}$$

$$\nabla \cdot \mathbf{v} = 0 \tag{10}$$

$$\frac{\partial T}{\partial t} + \mathbf{v} \cdot \nabla T = \nabla^2 T, \tag{11}$$

with the boundary conditions of impermeable and conducting lower and upper horizontal planes

$$w = T - 1 = 0, \quad z = -1/2, \tag{12}$$

$$w = T = 0, \quad z = 1/2. \tag{13}$$

Here the Rayleigh number R is defined as

$$R = \frac{\rho_0 g \beta K \Delta T h}{\mu \kappa_m}. \tag{14}$$

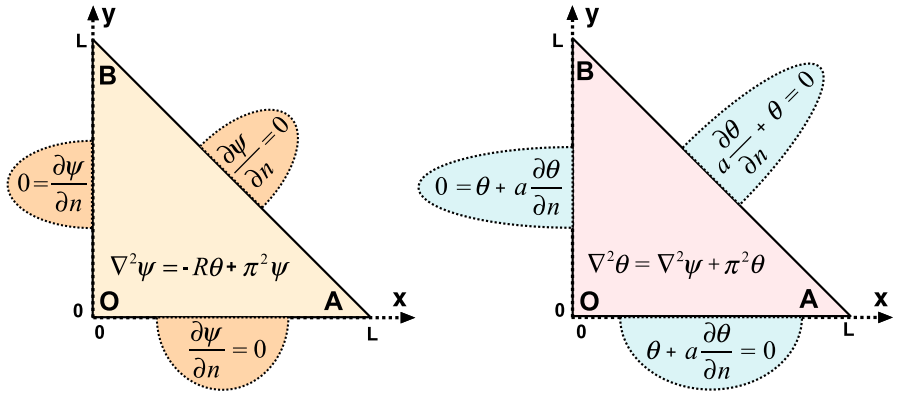

Fig. 2 Illustration of the governing equations and corresponding boundary conditions of the 2D coupled eigenvalue problem.

2.2 Basic solution

The stationary basic solution of eqs. (9)-(13) is given subscript "b".

$$\mathbf{v}_b = 0, \quad T_b = \frac{1}{2} - z, \quad P_b = \frac{1}{2} R\, z\,(1-z)\,. \tag{15}$$

This basic state has a linear temperature profile.

2.3 Linearized perturbation equations

In our stability analysis we disturb the basic state (15) with perturbed fields

$$\mathbf{v} = \mathbf{v}_b + \mathbf{v}, \quad T = T_b(z) + \Theta, \quad P = P_b(z) + p'. \tag{16}$$

where the perturbations $\mathbf{v}, \Theta, p'$ are functions of x, y, z and t. Linearizing eqs. (9)-(11) with respect to perturbations and eliminating the pressure gives

$$\nabla^2 w = R\nabla_1^2 \Theta, \tag{17}$$

$$\frac{\partial \Theta}{\partial t} - w = \nabla^2 \Theta. \tag{18}$$

We assume that the preferred flow at onset of convection is non-oscillatory. Then the heat equation (18) reduces to

$$-w = \nabla^2 \Theta. \tag{19}$$

Since the vertical component of the vorticity is zero, and the flow is incompressible, one single scalar function $\Psi(x, y, z)$ is sufficient for representing the entire 3D thermomechanical vector field. The velocity field is

$$\mathbf{v} = \nabla \times (\nabla \times \mathbf{k}\Psi), \tag{20}$$

where **k** is the unit vector in the vertical direction. The components of this vectorial relationship are

$$(u, v, w) = \left(\frac{\partial^2 \Psi}{\partial x \partial z}, \frac{\partial^2 \Psi}{\partial y \partial z}, -\nabla_1^2 \Psi \right), \tag{21}$$

where the operator $\nabla_1 = (\partial/\partial x, \partial/\partial y)$ has been introduced. The perturbation temperature is given by

$$\Theta = -R^{-1} \nabla^2 \Psi. \tag{22}$$

2.4 Degeneracy separating out the vertical direction

The thermomechanical conditions in the vertical direction makes the general cylinder problem degenerate in the vertical direction, as pointed out by Tyvand and Storesletten [6]. We can therefore write

$$\Psi(x, y, z) = \psi(x, y) \cos(\pi z), \tag{23}$$

$$\Theta(x, y, z) = \theta(x, y) \cos(\pi z), \tag{24}$$

already before we introduce the homogeneous boundary conditions at the vertical cylinder walls. Here we have picked only the most unstable mode in the vertical direction. The degeneracy in the vertical direction induces a common cosine variation which is the solution of the second-order Helmholtz equation for the vertical direction, replacing the full non-degenerate fourth-order differential equation. This degeneracy is a necessity to allow separability of the vertical dependency from the horizontal eigenfunction that we will study, with a full fourth-order dependency in the horizontal plane, not separable in x and y.

From eqs. (23) - (24) the thermomechanical eigenfunctions are expressed by the separated relationships

$$(u, v, w) = -\left(\pi \sin(\pi z) \frac{\partial \psi}{\partial x}, \pi \sin(\pi z) \frac{\partial \psi}{\partial y}, \cos(\pi z) \nabla_1^2 \psi \right), \tag{25}$$

$$\theta = R^{-1} (\pi^2 - \nabla_1^2) \psi, \tag{26}$$

after inserting the leading vertical normal mode ($n = 1$) into eqs. (21)-(22). It is physically consistent that the vertical variation of the horizontal velocity components have their maxima at the lower and upper boundaries. The corresponding maxima for the vertical velocity and the temperature perturbation are of course located in the middle of the layer, at $z = 1/2$. The theory that is developed so far, allows any mathematically consistent homogeneous thermomechanical condition to be posed at the cylinder walls.

2.5 Boundary conditions at cylinder walls

We will now introduce a choice of thermomechanical conditions at the vertical cylinder walls, without specifying the shape of the cylinder cross-section. As thermal boundary condition we take a general Robin condition

$$\theta + a\ \mathbf{n}\cdot\nabla\theta = 0, \quad \text{at the cylinder contour,} \tag{27}$$

where $a \geq 0$ is a dimensionless parameter of partial conduction. This condition was derived by Nygård and Tyvand [13], assuming that there is a thin cylindrical layer separating the thermoconvective flow domain of the porous cylinder from a surrounding medium that is perfectly conducting. As kinematic condition we take the simple condition of impermeable walls

$$\mathbf{n}\cdot\mathbf{v} = 0, \quad \text{at the cylinder contour,} \tag{28}$$

where $\mathbf{n}$ is the horizontal unit normal vector on the cylinder surface, pointing out from the porous cylinder.

3 The 2D eigenvalue problem

We will now formulate and solve the 2D eigenvalue problem for the horizontal perturbation temperature field $\theta(x,y)$ as it is coupled to the poloidal vector potential $\psi(x,y)$. The set of second-order governing equations is

$$(\nabla^2 - \pi^2)\psi + R\ \theta = 0, \tag{29}$$

$$\nabla^2\psi = (\nabla^2 - \pi^2)\theta. \tag{30}$$

which can be decoupled to give a fourth-order problem in $\psi(x,y)$ alone.

$$((\nabla^2 - \pi^2)^2 + R\nabla^2)\psi = 0, \tag{31}$$

where we now have omitted the subscript on the horizontal operator $\nabla = (\partial/\partial x, \partial/\partial y)$. We introduce the notation $\partial/\partial n = \mathbf{n}\cdot\nabla$. For the numerical solution procedure, it is preferable to keep the couplings between the eigenfunctions $\psi(x,y)$ and $\theta(x,y)$.

The thermal Robin condition is

$$\left(1 + a\frac{\partial}{\partial n}\right)\theta = 0, \quad \text{at the cylinder contour,} \tag{32}$$

while the kinematic condition of impermeable cylinder walls is

$$\frac{\partial\psi}{\partial n} = 0, \quad \text{at the cylinder contour.} \tag{33}$$

Hereby the general formulation is completed, before looking at a given cross-section shape. The circular shape with conducting wall has been treated by

Haugen and Tyvand [8], and extended to mixed (Robin-type) thermomechanical wall conditions by Nygård and Tyvand [9]. Bringedal *et al.* [14] have treated the case where the cylinder cross-section is a hollow circle. We are not aware of any previous publications that have analyzed non-circular cross-sections, with wall conditions that are incompatible with normal modes.

Figure 2 provides a definition sketch for the coupled eigenvalue problem that is valid in the 2D cross-section. The dimensionless parameters (aspect ratio L and Robin number a) are indicated in the sketch. Our analysis spans a wide variety of values for L and a, allowing physical realism for the non-degenerate fourth-order problem, in contrast to the inherent limitations of the previous normal-mode solutions. In particular, the conducting wall ($a = 0$) is the physically most important case, but we include other values of the Robin parameter (a), which also shows the transition to a case where the analytical solutions are well-known. Initially, we concentrate on the intermediate case $L = 1$ because it represents the preferred length scale of the classical HRL problem and highlights the differences between normal modes and non-normal modes.

4 Triangular cross-section

So far, we have developed a theory for the onset of convection in porous cylinders where the cross-section shape has not been specified. We are most interested in cases where analytical solutions exist for certain limit values of the Robin parameter a. Such solutions are of normal-mode type, and require that the fourth-order eigenvalue problem in the horizontal direction degenerates to a second-order problem governed by the Helmholtz equation. With the present model, this is possible only for the limit $a \to \infty$, where the wall conditions become compatible with normal modes. There are several classes of triangular cylinders where the Helmholtz equation has analytical solutions, but here we will consider only one case.

The thermal eigenfunctions show warm upwelling domains and cold downwelling domains of the cross-sectional plane. Strict upwelling as well as strict downwelling occur in stagnation points for the horizontal flow, defined by

$$|\nabla\psi| = 0, \tag{34}$$

which represents points with vanishing absolute value of the horizontal velocity vector. Graphically we introduce small green circles around the points where the velocity is purely vertical, as defined by eq. (34). The points of strict upwelling points must be located in the warm domains of positive temperature perturbation, but as we will see, pure upwelling does not coincide with a local maximum for the temperature perturbation. Only a normal-mode type solution will have strict upwelling or downwelling coinciding with extremal points for the temperature, which is implied by the eigenfunctions for the perturbation temperature and the vertical velocity being identical. Degeneracy

of the fourth-order eigenvalue problem to an essentially second-order problem is necessary to allow normal modes.

In the present paper, we will only study the right-angle isosceles triangle, which has simple analytical solutions of the Helmholtz equation, constituting normal modes, which in our case will be the valid limit solution for the limit of adiabatic walls $a \to \infty$.

The case of an equilateral cylinder can also be solved analytically for the normal-mode limit case $a \to \infty$. Such mathematical solutions have been established in the context of oscillating membranes.

4.1 The right-angle isosceles triangle

Tyvand and Storesletten [6] developed the simple normal-mode solutions for the right-angle isosceles triangle with boundary conditions that lead to degeneracy. The corners of the triangle in the x, y plane are termed O, A and B, with dimensionless coordinates $(0, 0)$ (the origin), $(L, 0)$ and $(0, L)$, respectively. Here L serves as the aspect ratio of the cylinder with a triangular cross-section.

We will now solve numerically the problem where the cylinder walls are impermeable with thermal Robin condition. No analytical solution exists for finite values of a, and we apply the commercial finite-element code Comsol Multiphysics. An eigenvalue solver with search algorithm estimates a pre-selected number of the adjacent eigenvalues around zero based on their convergence, and they are then classified based on their absolute eigenvalue number. The value $a = 0$ for the Robin parameter represents conducting cylinder wall. Figures 3 and 5 show the thermal eigenfunctions in the horizontal cross-section plane for $L = 1$, ordered according to their Rayleigh numbers of marginal stability. Figure 3 shows modes that are symmetric with respect to the mid-line that cuts the isosceles triangle in two smaller isosceles triangles. Figure 5 shows modes that are antisymmetric with respect to the same mid-line. We have not included full plots for the eigenfunctions of the flow, but we pick only the stagnation points for the horizontal flow, which are marked with small green circles. These circles represent points where the velocity field has only a vertical component. A green circle in a red domain represents a spot of strict upwelling, while a green circle in a blue domain represents a spot of strict downwelling. These green circles give hints concerning the physical significance of non-normal modes because any normal-mode solution for a vertical cylinder will give strict upwelling/downwelling exactly at the extremal points for the temperature perturbation.

Figures 4 and 6 provide immediate comparisons with the corresponding analogy solutions of the normal-mode type. These analogy solutions of the normal-mode type were derived by (Tyvand and Storesletten 2018), and are given by

$$\theta_{mn}(x, y) = \sin\frac{m\pi x}{L}\sin\frac{n\pi y}{L} - \sin\frac{m\pi(L-y)}{L}\sin\frac{n\pi(L-x)}{L}, \qquad (35)$$

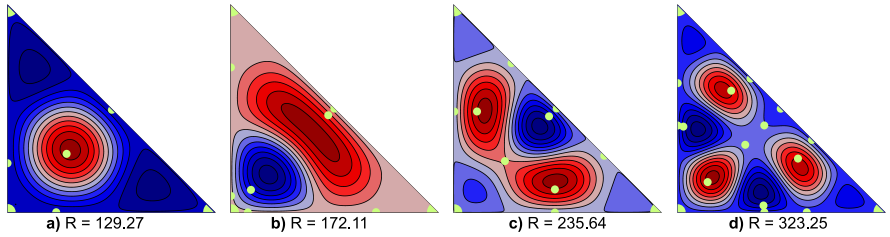

Fig. 3 Symmetric isotherms for conducting impermeable cylinder where $L = 1$. Plots are given in the order of increasing Rayleigh numbers (R). Green circles indicate points with zero horizontal velocity.

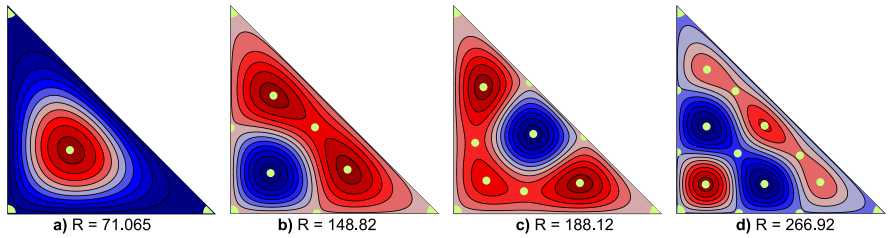

Fig. 4 Symmetric normal-mode eigenfunctions with Dirichlet wall conditions (L=1). The pair of horizontal mode numbers (m,n) are specified in each case. Green circles indicate points with zero horizontal velocity. **a)** $(m, n) = (1, 2)$, **b)** $(m, n) = (2, 3)$, **c)** $(m, n) = (1, 4)$, **d)** $(m, n) = (3, 4)$

where the mode numbers m and n are positive integers with $m \neq n$. Figure 4 gives the symmetric thermal eigenfunctions that are the normal-mode analogies of the symmetric non-normal mode solutions of Figure 3. Figure 6 gives the antisymmetric thermal eigenfunctions that are the normal-mode analogies of the antisymmetric non-normal mode solutions of Figure 5. These normal-mode solutions represent a conducting cylinder wall that is open to free flow in and out from a surrounding reservoir. See Barletta and Storesletten [7], who derived such normal-mode solution for a cylinder with an elliptical cross-section, where the cylinder walls are open and thermally conducting cylinder. The analogy solution (35) is a degenerate solution for a 4th order eigenvalue problem, in contrast to our numerical non-normal mode solution for an irreducible 4th order problem. The thermal conditions are the same for the exact problem and its analogy problem, which indicates that the respective thermal eigenfunctions may be comparable. There are no other differences than the mechanical conditions for the flow. The exact problem has impermeable cylinder walls, while the analogy problem of the normal-mode type has open cylinder walls where there is free flow in and out from a surrounding reservoir.

Each normal-mode type thermal eigenfunction θ_{mn} given in eq. (35) has the same shape as the corresponding eigenfunction for the vertical velocity distribution $w_{mn}(x, y)$ over the cross-section area, where the degeneracy represents cylinder walls that are open to a surrounding reservoir so that the w cancels along the triangular cylinder contour. The subscripts m and n refer

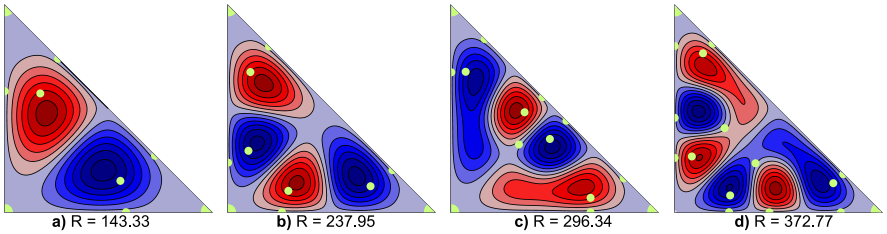

Fig. 5 Antisymmetric isotherms for conducting impermeable cylinder where $L = 1$. Plots are given in the order of increasing Rayleigh numbers (R). Green circles indicate points with zero horizontal velocity.

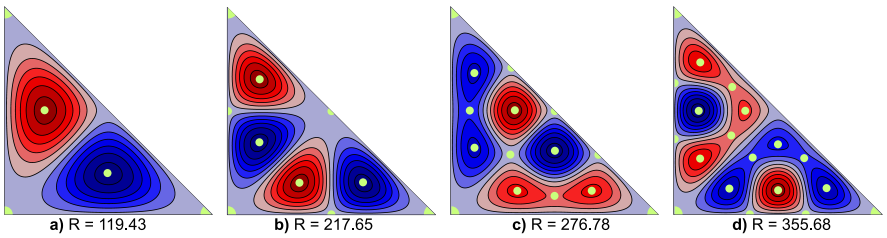

Fig. 6 Antisymmetric normal-mode eigenfunctions with Dirichlet wall conditions (L=1). The pair of horizontal mode numbers (m,n) are specified in each case. Green circles indicate points with zero horizontal velocity. **a)** $(m, n) = (1, 3)$, **b)** $(m, n) = (2, 4)$, **c)** $(m, n) = (1, 5)$, **d)** $(m, n) = (3, 5)$

to the two wave-number components in the x and y direction from which the normal-mode type solution is constructed.

No mode numbers exist for the non-normal mode solutions. It is therefore interesting to try to associate each non-normal mode with a corresponding normal-mode analogy. When we compare the symmetric modes in Figures 3 and 4, we find that only the first three modes are comparable. The antisymmetric modes in Figures 5 and 6 are more closely linked since each of the four displayed non-normal modes is reasonably analogous to its normal-mode counterpart. The analogy solution (35) is not useful for benchmarking. The comparisons in Figures 3-6 between non-normal modes and the normal modes of eq. (35) are merely analogies, without any benchmarking.

However, there is another normal-mode limit solution that we can use for quantitative benchmarking (Tyvand and Storesletten [6]),

$$\theta_{mn}(x, y) = \cos\frac{m\pi x}{L}\cos\frac{n\pi y}{L} + \cos\frac{m\pi(L-y)x}{L}\cos\frac{n\pi(L-x)}{L}, \qquad (36)$$

where the mode numbers m and n are non-negative integers, where $m+m > 0$. The legal solutions where either m or n is zero while the other one is a positive integer were erroneously excluded from the family of solutions displayed by Tyvand and Storesletten [6], so they are reintroduced in the present paper. This analytical normal-mode limit solution represents adiabatic impermeable walls, and it applies to our limit case $a \to \infty$. We will pick a number of values

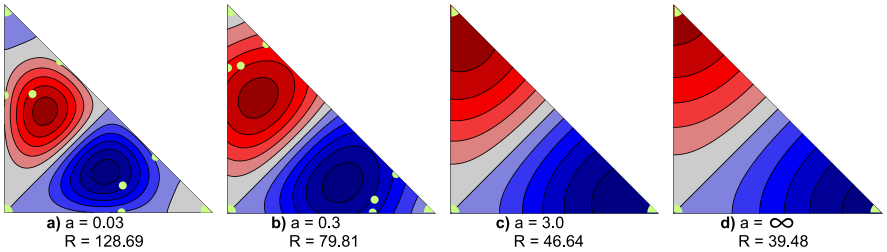

Fig. 7 Antisymmetric isotherms for conducting impermeable cylinder where $L = 1$. Plots are given in the order of increasing Robin number (a). Green circles indicate points with zero horizontal velocity.

for a to see how the thermal eigenfunctions gradually approach the known analytical limit solution (36) as a increases.

Benchmarking for the thermal eigenfunctions are visualized in Figures 7 and 8. Here we show the two eigenfunctions with the lowest Rayleigh number for $L = 1$, increasing the Robin parameter a, The value $a = 0$ is omitted here since it has already been displayed in Figure 3 (symmetric) and Figure 5 (antisymmetric). We display the eigenfunctions for the values $a = 0.03, 0.3, 3$ and $a = \infty$, where the last case is the normal-mode solution (36). Figure 7 shows the antisymmetric eigenfunction with the lowest value for R for each choice of a. Figure 8 shows the symmetric eigenfunction with the lowest eigenvalue for R, and it is smaller than the eigenvalue for the antisymmetric eigenfunction when a is small. When a is large, the situation changes so that the antisymmetric eigenfunction has the smallest eigenvalue for R and represents the preferred mode for the onset of convection.

Figures 7 and 8 show how the thermal eigenfunctions gradually change their nature with increasing Robin parameter a. At $a = 0$ we have the Dirichlet condition of zero perturbation temperature, while the limit $a = \infty$ is the Neumann-type adiabatic wall condition. The important qualitative change is that the isotherms are tangents to the boundary of the triangle at the lower (Dirichlet-type) limit $a = 0$ for the Robin parameter, while the isotherms are perpendicular to the boundary at the upper (Neumann-type) limit $a = \infty$.

As a increases, the green circles of upwelling/downwelling move from being off-centre of the local temperature maxima to coincide with these temperature maxima at $a = \infty$, which is the mathematically degenerate limit case where the solution is of normal-mode type. The Neumann condition of adiabatic walls causes all these temperature maxima to be located along the boundary of the triangle, as far as the two lowest modes are concerned.

We note that the type of onset eigenfunction that gives the critical Rayleigh number will vary when we vary the parameter a. It is known from earlier work that the shape of the eigenfunction will also vary with the horizontal side length L.

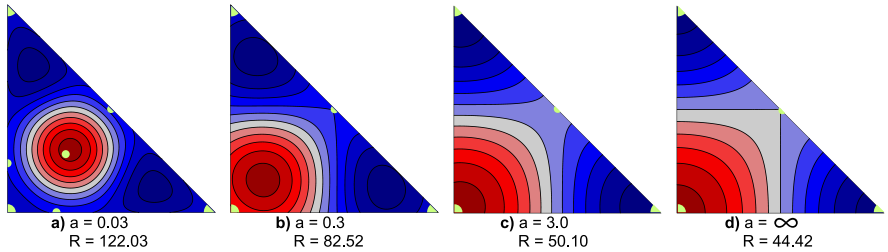

Fig. 8 Symmetric isotherms for conducting impermeable cylinder where $L = 1$. Plots are given in the order of increasing Robin number (a). Green circles indicate points with zero horizontal velocity.

4.1.1 The Rayleigh number at marginal stability

The critical Rayleigh number R_c as a function of L and a will now be calculated, for the chosen cross-section of a right-angle isosceles triangle. We have an analytical formula only for the asymptotic limit $a \to \infty$, given by

$$\sqrt{R_c} = \pi \min_{m,n} \left(\sqrt{\frac{m^2}{L^2} + \frac{n^2}{L^2}} + \left(\sqrt{\frac{m^2}{L^2} + \frac{n^2}{L^2}} \right)^{-1} \right), \tag{37}$$

being derived by Tyvand and Storesletten [6]. Again we must correct their application of this formula, noting that all nonzero combinations of the integers m and n are legal, as long as they are not both zero. This also means that the onset criterion (37) coincides exactly with the criterion for the onset of convection in cylinders with a square cross-section, which was given by Beck [4] as a subset of his general solution for a rectangular cylinder.

Figures 9-11 show how the Rayleigh number R at marginal stability decreases with increases Robin parameter a for increasing values of L. The numerical search looks for the five lowest Rayleigh numbers at each aspect ratio, and they are classified based on their absolute value. As a result, the curves will never overlap (even though the individual eigenfunctions switch between the different classifications). A general trend is that the Rayleigh number always decreases with increasing a, which is plausible since increasing a represents an enhanced loss of heat by conduction through the impermeable cylinder walls. Loss of heat reduces the buoyancy that drives the flow, which explains why the marginal Rayleigh number decreases with increasing a.

Figure 9 represents a slender cylinder with $L = 1/3$, where the Rayleigh numbers are large when the wall is highly conductive (small a). Figure 10 shows the case $L = 1$, which has served as a reference case in our investigations above. We know from Tyvand and Storesletten [6] that the classical value $R_c = 4\pi^2$ appears for $L = 1$, but only in the limit $a \to \infty$, for the lowest mode. This result is confirmed in Figure 7 (d). Figure 11 shows a short cylinder with $L = 3$, where the Rayleigh number is small for a number of modes since the modes become almost periodic when the length scale of the triangle exceeds the length scale of the preferred modes.

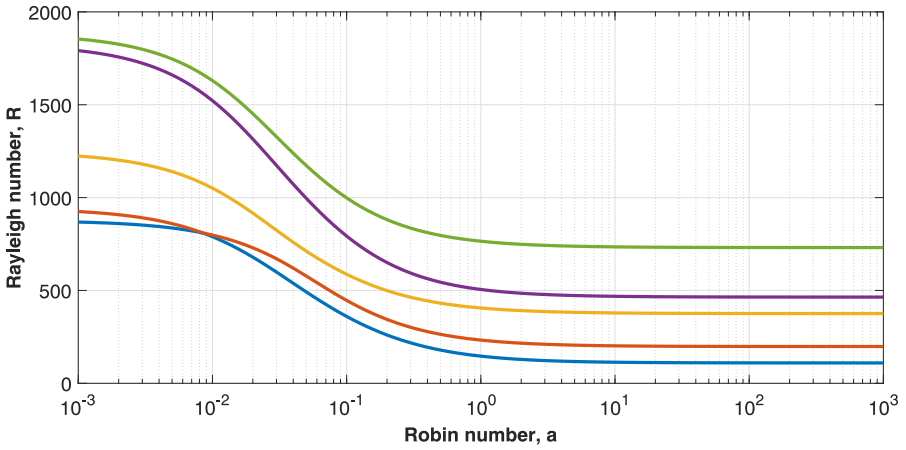

Fig. 9 Numerical search of the 5 lowest Rayleigh numbers as a function of the Robin number with aspect ratio $L = 1/3$. The x-axis has a logarithmic scale.

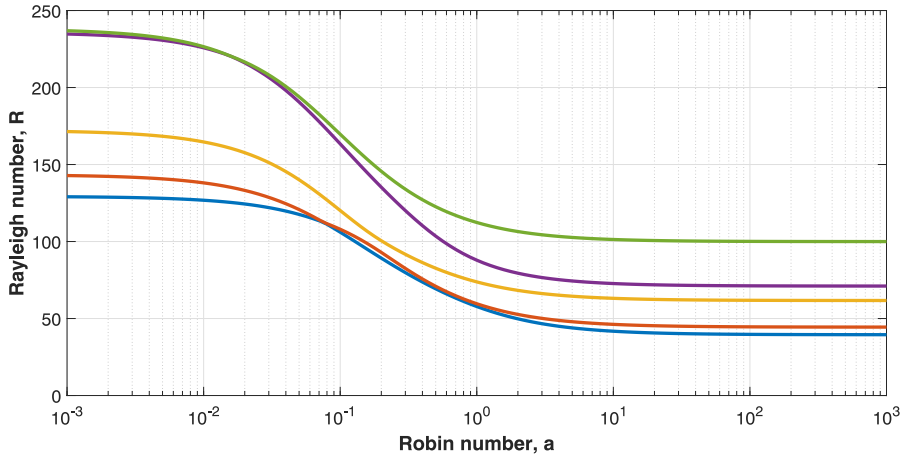

Fig. 10 Numerical search of the 5 lowest Rayleigh numbers as a function of the Robin number with aspect ratio $L = 1$. The x-axis has a logarithmic scale.

Figures 12-14 show how the Rayleigh number at marginal stability varies with the aspect ratio L for three given values of the Robin parameter of partial conduction (a). Figure 12 represents $a = 0$, which is the case of a conducting cylinder wall. The same condition for a circular cylinder was studied by Haugen and Tyvand [8], and we note the important differences between the circle and our triangle. The circular case allows separation of variables in the azimuthal and radial directions. The ordinary differential equation in the radial direction is solvable analytically for circular geometry, while no analytical methods are known for the same eigenvalue problem for the triangle.

Haugen and Tyvand [8] found that the axisymmetric mode is preferred for all aspects ratios when the cylinder cross-section is circular. Our correspond-

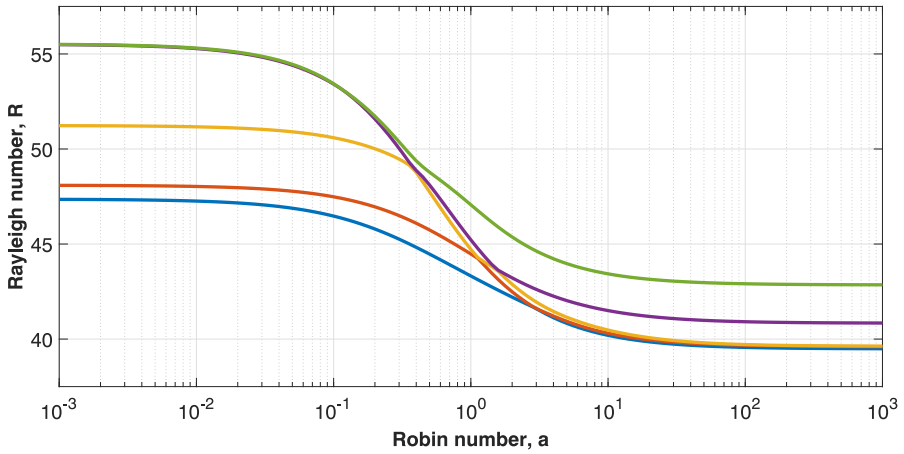

Fig. 11 Numerical search of the 5 lowest Rayleigh numbers as a function of the Robin number with aspect ratio $L = 3$. The x-axis has a logarithmic scale.

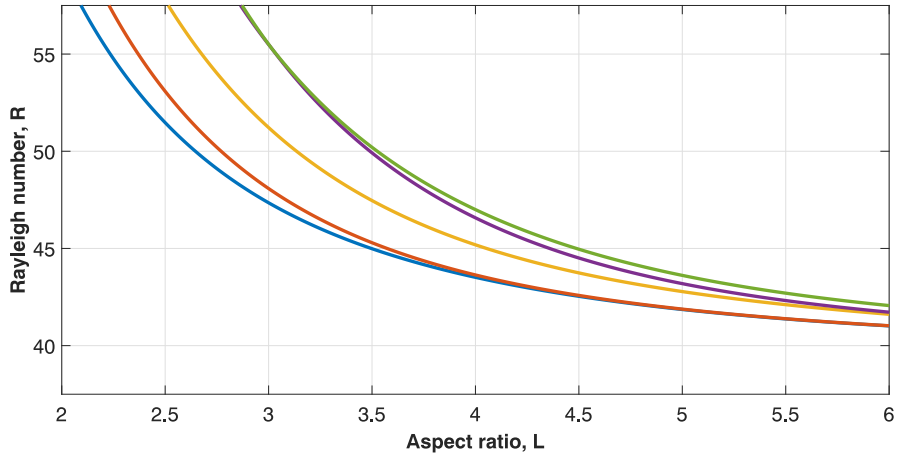

Fig. 12 Numerical search of the 5 lowest Rayleigh as a function of the aspect ratio (L) at zero Robin number, $a = 0$ (fully conducting impermeable wall).

ing Figure 12 does not have a similar possibility since there is no such thing as axisymmetry for a triangular cross-section. Therefore, the type of mode that is preferred will vary with the parameter values of a and L, which is revealed in Figures 9-14. The numerical method does not track the individual onset modes when L varies in Figures 12-14, but picks the five lowest modes for each parameter choice. Therefore we see that individual solution branches cross one another several places, even though this fact is disguised by truncation errors in the numerical method. Tyvand *et al.* [12] misinterpreted these numerical truncation errors, and stated that the individual modes do not cross one another in the diagrams of the marginal Rayleigh number as a function of

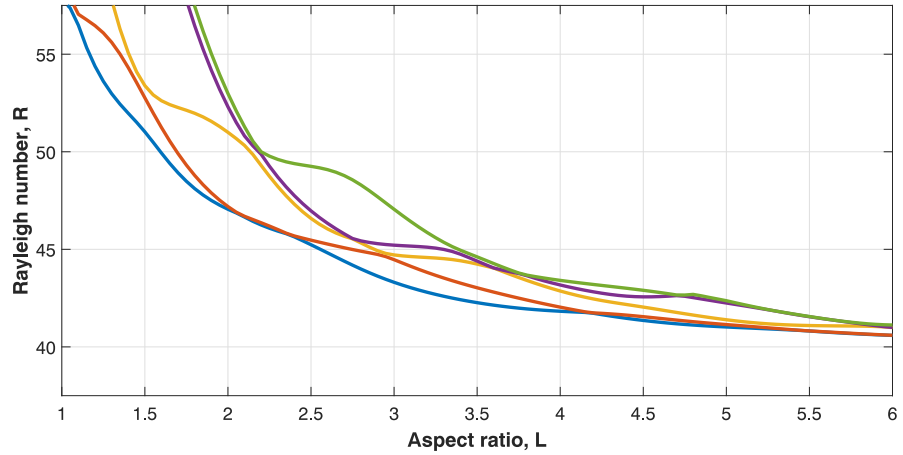

Fig. 13 Numerical search of the 5 lowest Rayleigh numbers as a function of the aspect ratio (L) at unity Robin number, $a = 1$ (partially conducting impermeable wall).

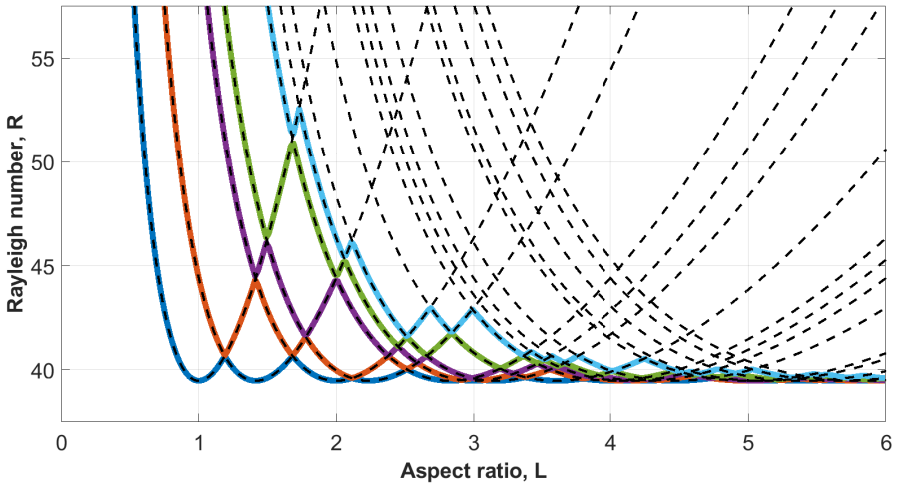

Fig. 14 Numerical search of the five lowest Rayleigh numbers as a function of the aspect ratio (L) at infinite Robin number, $a = \infty$ (fully insulating impermeable wall). Comparison is made with coinciding analytical solutions (Tyvand and Storesletten 2018), which extend the curves of the numerical solutions.

L. Figure 13 gives a clear indication of the individual curves for non-normal modes will cross one another, for the case of partial conduction where $a = 1$. The final case of Figure 14 is $a = \infty$, which coincides with the second case (Neumann condition) of the normal-mode solutions displayed by Tyvand and Storesletten [6]. The calculated cases of the five lowest eigenmodes are complemented with dashed curves from Tyvand and Storesletten [6], represented in the present paper by eq. (37). Again we make the correction that all combinations of non-negative integers m and n where the sum $m + n > 0$ must

be included. With this correction, the present results agree almost fully with Tyvand and Storesletten [6], apart from the small gaps that arise in these plots at the points where the graphs of individual normal modes cross one another. The analytical theory has proven that these individual curves cross one another. Since the dependency of a is smooth as far as the Rayleigh number is concerned, we find it likely that individual non-normal modes also cross one another in many occasions.

Figures 7 and 8 above have already identified such a case, where an antisymmetric onset mode takes over for the symmetric mode as the most unstable onset mode as the Robin parameter a exceeds a value of order 0.1. We do not give the exact value for a above which the antisymmetric non-normal mode takes over, but find it sufficient to compute the marginal Rayleigh numbers at $a = 0.1$: The symmetric mode gives $R = 107.95$, while the antisymmetric mode $R = 106.05$. These numbers are fairly close to one another, showing that the switch to antisymmetric has already taken place, at a value of a slightly below 0.1.

5 Summary and conclusions

The topic of the present paper is the fourth-order Darcy-Bénard eigenvalue problem for the onset of thermal convection in a vertical porous prism with impermeable walls. The three-dimensional problem is analyzed numerically in a reduced two-dimensional form. The conditions of impermeable upper and lower boundaries kept at constant temperatures separate out the vertical dependency, resulting in a 2D eigenvalue problem for the cross-section of the enclosure. A Robin-type thermal boundary condition of partial conduction is applied at the cylinder wall.

A general formulation is given for an arbitrary cross-section of the vertical cylinder, but numerical computations are given only for a triangular isosceles right-angle cross-section. The non-normal mode eigenfunctions gradually change their physical nature as the Robin parameter of partial conduction increases. In the limit of infinite Robin parameter, the solution converges to the normal-mode solution known from Tyvand and Storesletten [6]. This is the standard Neumann condition of a thermally insulating wall, first investigated by Wooding [3].

The non-normal mode behaviour of the thermal eigenfunctions for the triangular porous cylinder displaces the horizontal stagnation points away from the extremal points of the temperature perturbation. In fact, these displacements are qualitatively significant, since a normal-mode dependency in the horizontal cross-section domain will generate zero horizontal velocity exactly at the extremal points for the temperature perturbation. Moreover, at these stagnation points for the horizontal velocity, the velocity is vertical. They may represent either a hot spot of upwelling or a cold spot of downwelling.

The critical Rayleigh number decreases with increasing value of the Robin parameter value for all the cases investigated. This is plausible because enclo-

sure walls with higher Robin parameter have the destabilizing effect of reduced heat loss. The critical Rayleigh number varies smoothly with the aspect ratio in the fully conducting wall case, but irregularities are observed as the Robin parameter increases.

The presented results in this paper have been validated from two types of cases where known analytical normal-mode solutions exist. First, a qualitative comparison of the eigenfunctions for a conducting wall is provided. We highlight them to cover the similarities with the discrete Fourier mode numbers that constitute a normal mode solution. Next, a benchmarking comparison is made with the normal-mode solution, which is asymptotically valid for infinite Robin parameter.

Earlier work on vertical porous cylinders with fully or partly conducting boundaries have been restricted to circular geometries where the problem separates in space, leading to a one-dimensional eigenvalue problem in the horizontal radial direction. With a triangular cross-section, the horizontal eigenfunction is a non-normal mode.

The present analysis provides new scientific insights regarding the behaviour of non-normal modes of convection in a triangular cross-section of a porous prism. This is one of the few geometries where normal modes have a simple analytical form, while the convection problem is non-separable and cannot be solved analytically. It proved useful to apply a thermal Robin condition for utilizing the benchmarking possibilities of an analytical solution for the 2D Helmholtz equation that constitutes normal modes.

In summary, the paper covers the following findings in this study of the triangular porous enclosure:

- Displacements of the stagnation points in the non-normal mode regime.
- Critical Rayleigh number and eigenfunction dependence of the degree of partial conduction at the wall boundaries for different aspect ratios.
- Critical Rayleigh number dependency of the aspect ratio of the cylinder for different degrees of partial conduction at the wall boundaries.
- Qualitative and quantitative validations from well known analytical theory.

References

1. Horton, C.W. and Rogers, F.T. (1945) Convection currents in a porous medium. J. Appl. Phys. **16**, 367-370.
2. Lapwood, E.R. (1948) Convection of a fluid in a porous medium. Proc. Camb. Phil. Soc. **44**, 508-521.
3. Wooding, R.A. (1959) The stability of a viscous liquid in a vertical tube containing porous material. Proc. R. Soc. Lond. **A252**, 120-134.
4. Beck, J.L. (1972) Convection in a box of porous material saturated with fluid. Phys. Fluids **15**, 1377-1383.
5. Zebib, A. (1978) Onset of natural convection in a cylinder of water saturated porous media. Phys. Fluids **21**, 699-700.
6. Tyvand, P.A. and Storesletten, L. (2018) Degenerate onset of convection in vertical porous cylinders. J. Eng. Math. **133**, 633-651.
7. Barletta, A. and Storesletten, L. (2015) Onset of convection in a vertical porous cylinder with a permeable and conducting side boundary. Int. J. Therm. Sci. **97**, 9-16.

8. Haugen, K.B. and Tyvand, P.A. (2003) Onset of thermal convection in a vertical porous cylinder with conducting wall. Phys. Fluids **15**, 2661-2667.
9. Nygård, H. S. and Tyvand, P.A. (2011) Onset of Thermal Convection in a Vertical Porous Cylinder with a Partly Conducting and Partly Penetrative Cylinder Wall. Transp. Porous Med. **86**, 229-241.
10. Nield, D.A. (1968) Onset of thermohaline convection in a porous medium (appendix). Water Resources Res. **11**, 553-560.
11. Barletta, A., Tyvand, P.A. and Nygård, H.S. (2015) Onset of convection in a porous layer with mixed boundary conditions. J. Eng. Math. **91**, 105-120.
12. Tyvand, P.A., Nøland, J.K. and Storesletten, L. (2019) A non-normal-mode marginal state of convection in a porous rectangle. Transp. Porous Med. **128**, 633-651,
13. Nygård, H. S. and Tyvand, P.A. (2010) Onset of convection in a porous box with partly conducting and partly penetrative sidewalls. Transp. Porous Med. **84**, 55-73.
14. Bringedal, C., Berre, I., Nordbotten, J.M ,Rees, D.A.S. (2011) Linear and nonlinear convection in porous media between coaxial cylinders. Phys. Fluids. **23**,094109